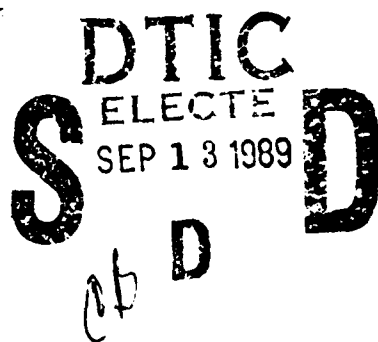


AD-A212 479



2

APPLICATION OF REMOTE SENSING OPTICAL INSTRUMENTATION
FOR DIAGNOSTICS AND SAFETY OF NAVAL STEAM BOILERS

Navy Contract #N00014-87-K-0056
Final Technical Report
July 1989

Prepared By The
Diagnostic Instrumentation and Analysis Laboratory
(formerly MHD Energy Center)
Mississippi State University
Mississippi State, Mississippi 39762

DISTRIBUTION STATEMENT A
Approved for public release
Distribution Unlimited

TABLE OF CONTENTS

| | |
|---|-----|
| List of Figures. | iii |
| Summary. | 1 |
| Facilities | 2 |
| Diagnostic Instrumentation | 4 |
| Fuel Sensor. | 4 |
| UV-Visible Spectroscopy. | 10 |
| Cross Correlation Flame Monitor | 10 |
| Soot Temperature Measurements | 18 |
| Infrared Spectroscopy | 19 |
| HeNe Differential Infrared Hydrocarbon Monitor. | 19 |
| Diode Laser CO/CO2 Monitor. | 29 |
| Auxiliary Instrumentation | 30 |
| Bench-Top Fuel-Oil Burner | 30 |
| Explosion Test Cell | 31 |
| Gas and Liquid Chromatography | 34 |
| Conclusions. | 36 |
| References | 37 |
| Appendix | 38 |
| Publications and Presentations | 39 |



| | |
|--------------------|-------------------------------------|
| Accession For | |
| NTIS - CRA&I | <input checked="" type="checkbox"/> |
| DTIC - TAB | <input type="checkbox"/> |
| Unannounced | <input type="checkbox"/> |
| Justification | |
| By <i>per ltr</i> | |
| Distribution | |
| Availability Codes | |
| Dist | Avail and/or Special |
| A-1 | |

LIST OF FIGURES

| | | |
|-----|--|----|
| 1. | Fuel sensor detection circuit. | 5 |
| 2. | Frequency variation with Korundal Fine Plastic refractory bricks . | 7 |
| 3. | Steady state detector output voltage with Korundal Fine Plastic refractory bricks. | 8 |
| 4. | Detector circuit voltage response to 5 cc fuel addition steps. . . | 9 |
| 5. | Average signal intensity as a function of wavelength | 12 |
| 6. | Signal intensity as a function of time | 13 |
| 7. | The time-varying signal has been Fourier transformed into the frequency domain | 15 |
| 8. | Optical arrangement for the cross-correlation technique. | 16 |
| 9. | Correlation between the two signals over a frequency range of 400-500 Hz | 17 |
| 10. | A longitudinal cross section of the combustor and the boiler simulator section. | 20 |
| 11. | Relative radiation intensity as a function of wavelength for two different equivalence ratios | 21 |
| 12. | Experimental spectrum transformed into $\log (I/\lambda^6)$ versus C_2/λ coordinates | 22 |
| 13. | Schematic diagram of the HeNe differential infrared (hydrocarbon) monitor. | 24 |
| 14. | Experimental data record showing the absorption by 0.2 torr methane in a 10-cm cell. | 25 |
| 15. | Methane concentration distribution in a bench-top methane flame. | 27 |
| 16. | Absorption of methane in the test stand at different air flow rates (300 lb/hr and 100 lb/hr). | 28 |
| 17. | Bench-top fuel oil burner. | 32 |
| 18. | Detailed diagram of the explosion test cell. | 33 |

SUMMARY

Diagnostic sensors for monitoring the flame (flame quality), the air/fuel ratio, the presence of unburned hydrocarbon vapors, and the presence of liquid fuel on the floor of a burner are under development. Because safety and burner efficiencies are related to these conditions, sensors whose designs have been aimed at improving safety conditions can simultaneously be used to study efficiencies.

Several techniques for evaluating the operating conditions of boiler flames are currently under investigation at the Diagnostic Instrumentation and Analysis Laboratory (DIAL) of Mississippi State University. These include a capacitance-based liquid monitoring system and optical experiments for monitoring flame quality, hydrocarbon vapors, and the CO/CO₂ ratio in the effluent gases. Each of these techniques is designed to be used in the flame region of a boiler. The optical experiments can be tested using bench-top natural gas or fuel oil burners, a small explosion test cell, or a combustion test facility (CTF) which is maintained and operated by the laboratory. This range of combustion media allow development and testing in a laboratory environment as well as in environments which more closely approximate the conditions of a Navy boiler. Additional scale-up and evaluation will be necessary before the equipment can be conveniently mounted on a boiler or boiler simulator.

FACILITIES

The Diagnostic Instrumentation and Analysis Laboratory (DIAL) at Mississippi State University (MSU) maintains and operates a fuel oil-fired combustion test facility (CTF) which has been used for a series of scale-up tests employing some of the instrumentation developed. This facility consists primarily of a computer-controlled test stand which was designed to be flexible in simulating various gas stream and combustion conditions. The following conditions, which have been useful in the development of naval boiler diagnostics, can be safely simulated on the DIAL test stand:

- * Steady-state combustion with air/fuel ratios in the range of approximately 0.75 to 1.50,
- * Poor fuel atomization, and
- * Water in the fuel.

Some of the other conditions which can lead to potentially explosive conditions might also be simulated on this test stand, although it is not clear at this time as to what safety hazards might be produced.

A combustor is on hand which burns fuel oil with or without preheating the combustion air. Test sections with optical pathlengths of up to approximately 20 inches and fitted with optical ports for viewing both through and behind the flame are also available.

This test facility is well-suited for performing a variety of combustion-related experiments because of the ability to provide precisely known air/fuel ratios and gas stream flowrates. However, many of the gas stream conditions necessary for testing naval boiler instrumentation are impossible to simulate or are too dangerous since the DIAL test stand was designed to operate under steady-state conditions.

At some point in the future, the diagnostic instrumentation will have to be tested in a naval boiler simulator capable of safely operating under the following hazardous conditions:

- * Unburned fuel on the firebox floor,
- * Atomizer malfunctions,
- * Atomizing steam problem,

- * Air/fuel ratio problems,
 - Excess combustion air ("white-smoke condition"),
 - Insufficient combustion air ("black-smoke condition"),
- * Water in fuel oil, and
- * Loss of flame.

DIAGNOSTIC INSTRUMENTATION

Fuel Sensor

In an effort to develop a detector that would measure the presence of unburned fuel oil in a naval boiler two types of fuel sensors were explored. The initial effort was directed toward adapting a resistive surface moisture monitor such as one described in a JPL Invention Report.¹ Laboratory testing produced unreliable results which were also less sensitive than originally anticipated. This technique was then abandoned as infeasible for the conditions of a boiler.

A more practical detector for unburned fuel oil has proven to be a capacitive sensor. The principle of operation is the change in the dielectric constant of a refractory brick due to the presence of fuel oil. Two porous refractory bricks with embedded parallel plates, each forming a capacitor, were fabricated. The refractory being used in these plates was Korundal Fine Plastic, manufactured by Harbison-Walker Refractories, Pittsburgh, PA. Thermal and other properties of this refractory are:

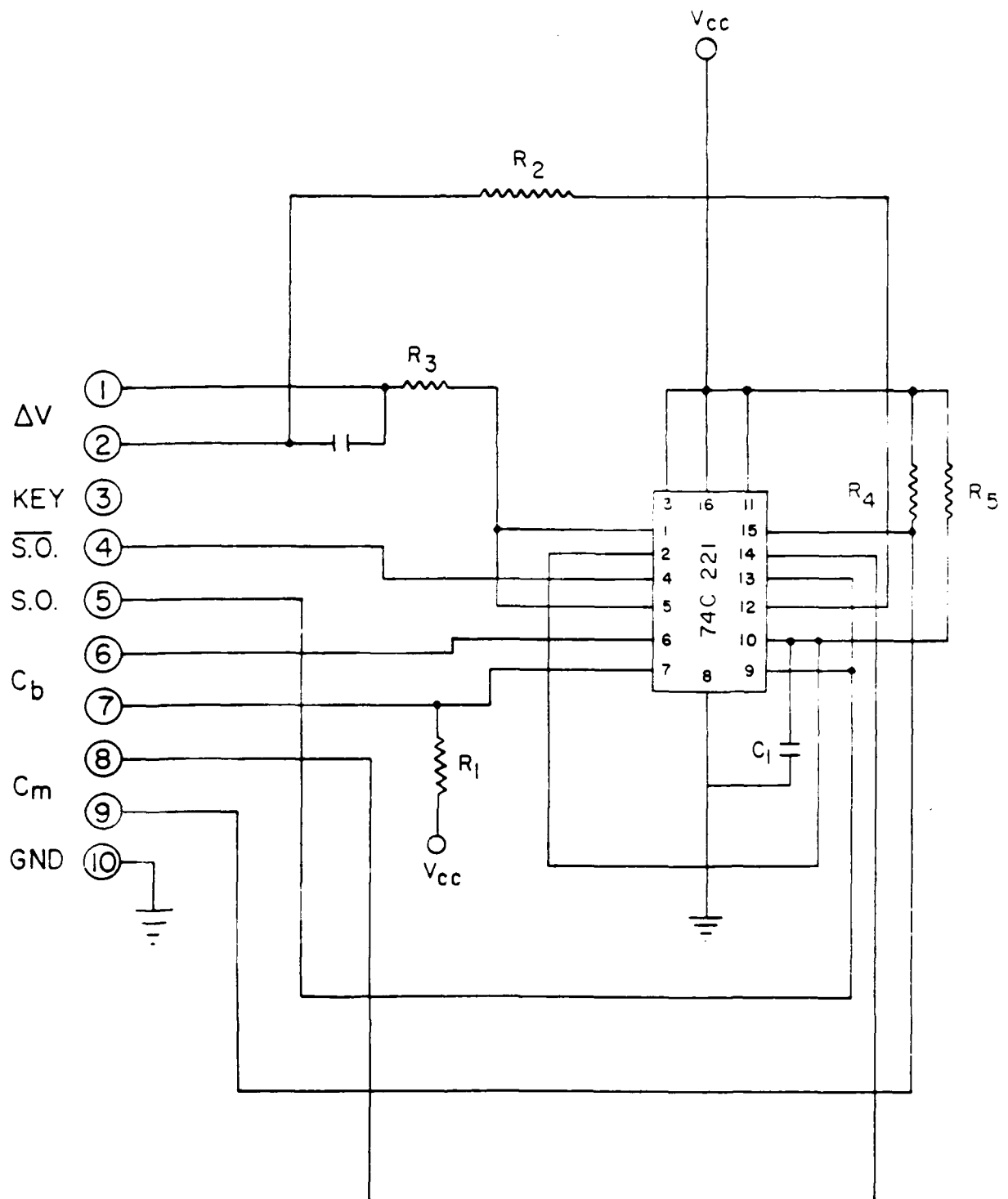
Max service temperature = 3300°F

Bulk density after drying = 182 lbs/cu.ft.

Primary applications: Broad application for very severe service;
soaking pit bottoms and slaglines; transfer
ladles; etc.

One of the bricks is used as the measurement brick and the other brick is used as a dry balancing capacitor in order that the effects of temperature and other thermal variation in the boiler may be minimized. It is anticipated that in a naval boiler, the measurement brick would be placed on the floor of the boiler and the balancing capacitive brick would be mounted on the walls or ceiling to prevent its exposure to unburned liquid fuel.

The detection circuit (Figure 1) consists of a dual multivibrator in which the two bricks replace the timing capacitors. The output of the circuit is a square wave with the up time controlled by the capacitance of one brick and the down time controlled by the capacitance of the other. The duty cycle of the



C_m = Measured capacitive brick

C_b = Balancing capacitive brick

ΔV = Detector voltage output

S.O. & $\overline{S.O.}$ = Square wave signal outputs

Figure 1. Fuel sensor detection circuit.

square wave is used to detect a capacitance change. The voltage across terminals (1) and (2) in Figure 1 is proportional to the change in duty cycle. This is the most sensitive indication of a capacitive change.

A computer circuit was designed and constructed to measure the actual difference in up and down times from the multivibrator. An MC68705PC single chip computer which has built-in EPROM memory was used. Measurements of the difference between up and down times to within one microsecond were made. This was not accurate enough for the present development work. It will likely be expanded in later work to measure the brick temperature and other parameters that affect the fuel sensor performance.

Table 1 shows the effect of fuel oil addition to one brick. Figure 2 shows the frequency variation of the square wave signal with fuel oil addition and Figure 3 shows the detector circuit's steady state, voltage change with fuel oil addition. Figure 4 shows a typical temporal variation of this voltage change.

Table 1. Effect of fuel oil addition on detector outputs.

| No. | Fuel added (cc) | Voltage V | Frequency KHz | Signal Width (micro secs) | |
|-----|--------------------|--------------|------------------|------------------------------|-----------|
| | | | | Up time | Down time |
| 1 | 0 | 0.1034 | 23.920 | 21.704 | 20.105 |
| 2 | 0 | 0.1033 | 23.916 | 21.707 | 20.109 |
| 3 | 5 | 0.0822 | 23.803 | 21.705 | 20.297 |
| 4 | 5 | 0.0625 | 23.699 | 21.719 | 20.477 |
| 5 | 5 | 0.0420 | 23.591 | 21.725 | 20.668 |
| 6 | 5 | 0.0274 | 23.493 | 21.730 | 20.839 |
| 7 | 5 | 0.0084 | 23.414 | 21.734 | 20.979 |
| 8 | 5 | -0.0087 | 23.324 | 21.738 | 21.138 |
| 9 | 5 | -0.0251 | 23.237 | 21.743 | 21.294 |
| 10 | 10 | -0.0615 | 23.044 | 21.754 | 21.645 |
| 11 | 10 | -0.0845 | 22.923 | 21.760 | 21.869 |
| 12 | 10 | -0.1077 | 22.801 | 21.767 | 21.097 |
| 13 | 10 | -0.1269 | 22.702 | 21.770 | 22.281 |

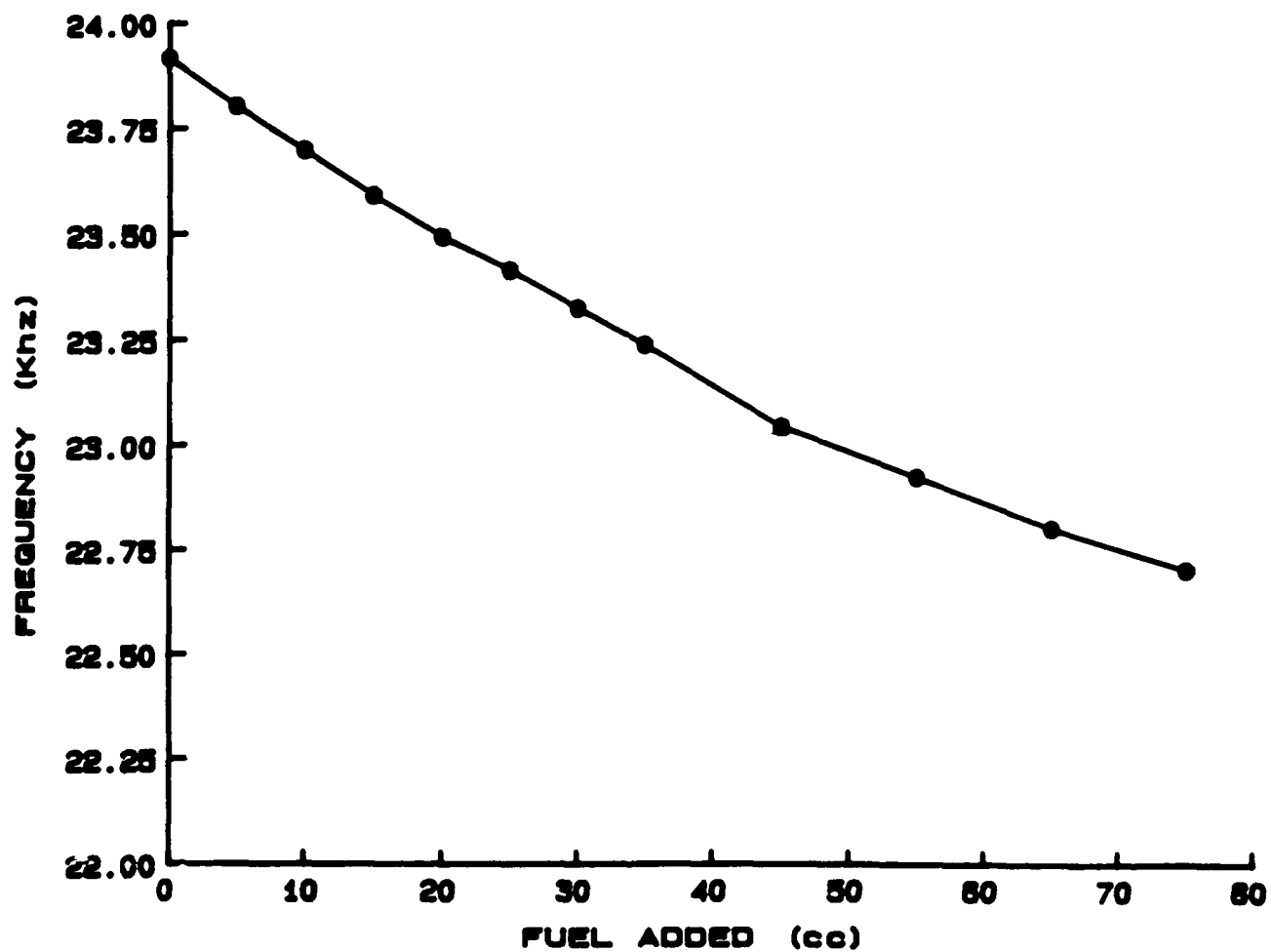


Figure 2. Frequency variation with Korundal Fine Plastic refractory bricks.

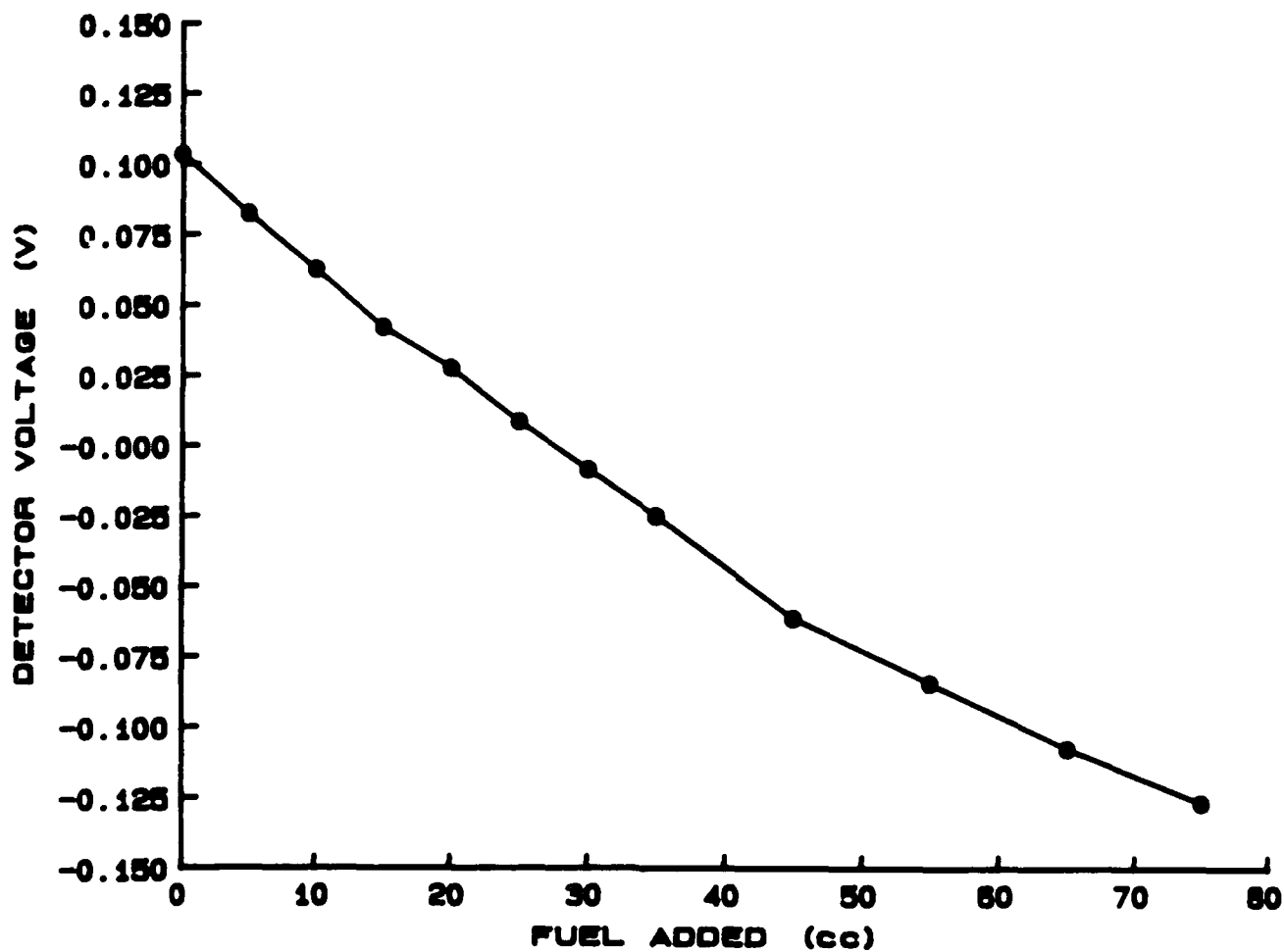


Figure 3. Steady state detector output voltage with Korundal Fine Plastic refractory bricks.

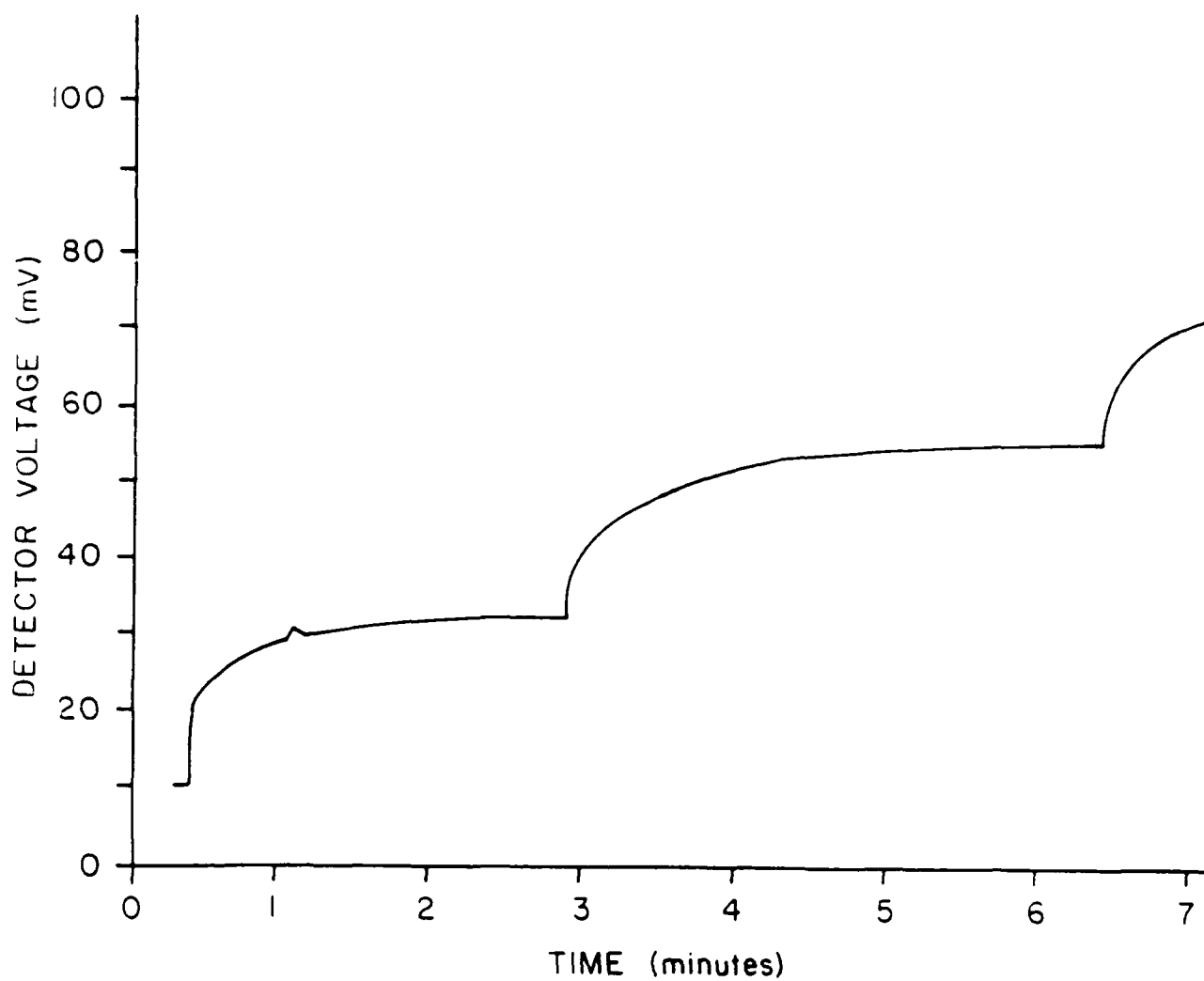


Figure 4. Detector circuit voltage response to 5 cc fuel addition steps.

The previous report² described some of the results obtained with the lightweight castable refractories. The results showed the temporal variation of detector output voltage with fuel oil addition. This figure showed the edge effect of having fuel oil sitting on the top of the brick before absorption. Maximum detector voltage was obtained at this point and the voltage dropped off exponentially as the fuel oil was gradually absorbed into the brick. Although the response time of this brick design is the shortest, there is an undesirable feature in that the brick would be very susceptible to humidity variations and other noise sources on top of the brick. This could very well mask the actual detection of fuel oil on the brick. To change this feature the current brick design has refractory filled over the top edges of the plates. The effect of this change in design is shown by the change of the brick response in Figure 4. In effect the capacitance of the brick increases to a steady state value as all the fuel oil is absorbed. There is no peak obtained as in the previous cases reported.

The basic electrical circuit for this measurement has been completed. The refractory brick has been tested under atmospheric conditions and is ready to be tested under firing conditions. Significant changes in voltage have been measured under atmospheric conditions. These changes in voltage (230 mV for 75 cc of fuel added to about 18 sq.in. of exposed brick surface area) are easily measurable. The problem, however, will be more difficult at elevated temperatures where the changes in dielectric constant might be brought about by rapidly changing temperatures at firing conditions. The change in brick design that has now been incorporated should, however, decrease those effects.

The technique so far seems to be a reliable indicator of fuel oil absorption. Its response is good enough and fast enough to be used under practical conditions. Further testing required includes boiler on/off conditions, variations in chamber testing conditions, and other scenarios in which this detector might be used.

UV-Visible Spectroscopy

Cross Correlation Flame Monitor: Current commercial flame detectors use the light emitted by a flame to verify the presence of the flame. However, this light is a complicated phenomenon and contains much information about the combustion process within the flame. This emitted light consists of different wavelengths of radiation, from the ultraviolet to the infrared. Due to turbulence

and other factors, the emitted radiation varies with time, containing fluctuations over a wide range of frequencies. Finally, the radiation is not spatially constant, varying from the base of the flame to the tip.

Therefore, as part of the research performed under this contract, development of a flame monitor was begun to more fully exploit the enormous information available in the light emitted by a flame. The ultimate objective is a robust, simple, passive flame monitor which is capable of increasing order of difficulty:

1. Adequate spatial resolution to detect loss-of-flame on an individual burner in a naval boiler;
2. Detection of abnormal, unsteady, or irregular combustion which might lead to loss-of-flame; and
3. Measurement, by purely optical means, of the fuel/air ratio of an individual burner, thus allowing automatic control of the fuel/air ratio.

The first phase of activity on this project concentrated on development of a bench-top optical flame monitor, flexible enough to analyze all aspects of the light emitted by a flame. The system has been tested on a bench-top, methane-air flame to verify its proper operation. This system can analyze the light according to wavelength, flicker frequency, and spatial location.

Studies of flames in premixed gases indicate that the relative intensities of different wavelengths of light are an accurate indicator of the fuel/air ratio.^{3,4} Thus, the fuel/air ratio could be determined by measuring the radiation intensity at two different wavelengths and taking the ratio of the two intensities. McArthur, et al., reported success with this method on industrial oil-fired boilers.⁵

The prototype flame monitor built at Mississippi State University incorporates wavelength sensitivity by means of a monochromator coupled to a photomultiplier tube detector, allowing the selection of any wavelength in the range 200-800 nm. Figure 5 is a graph of mean light intensity as a function of wavelength. Several peaks are clearly visible. These peaks can be assigned to radicals such as OH, CH and C₂ which are formed during combustion.

Figure 5 was produced by time averaging the output from the photomultiplier tube for each wavelength setting of the monochromator. If this signal is plotted as a function of time, the result is shown in Figure 6. The detector output varies with time, principally as a result of turbulence in the flame. A better

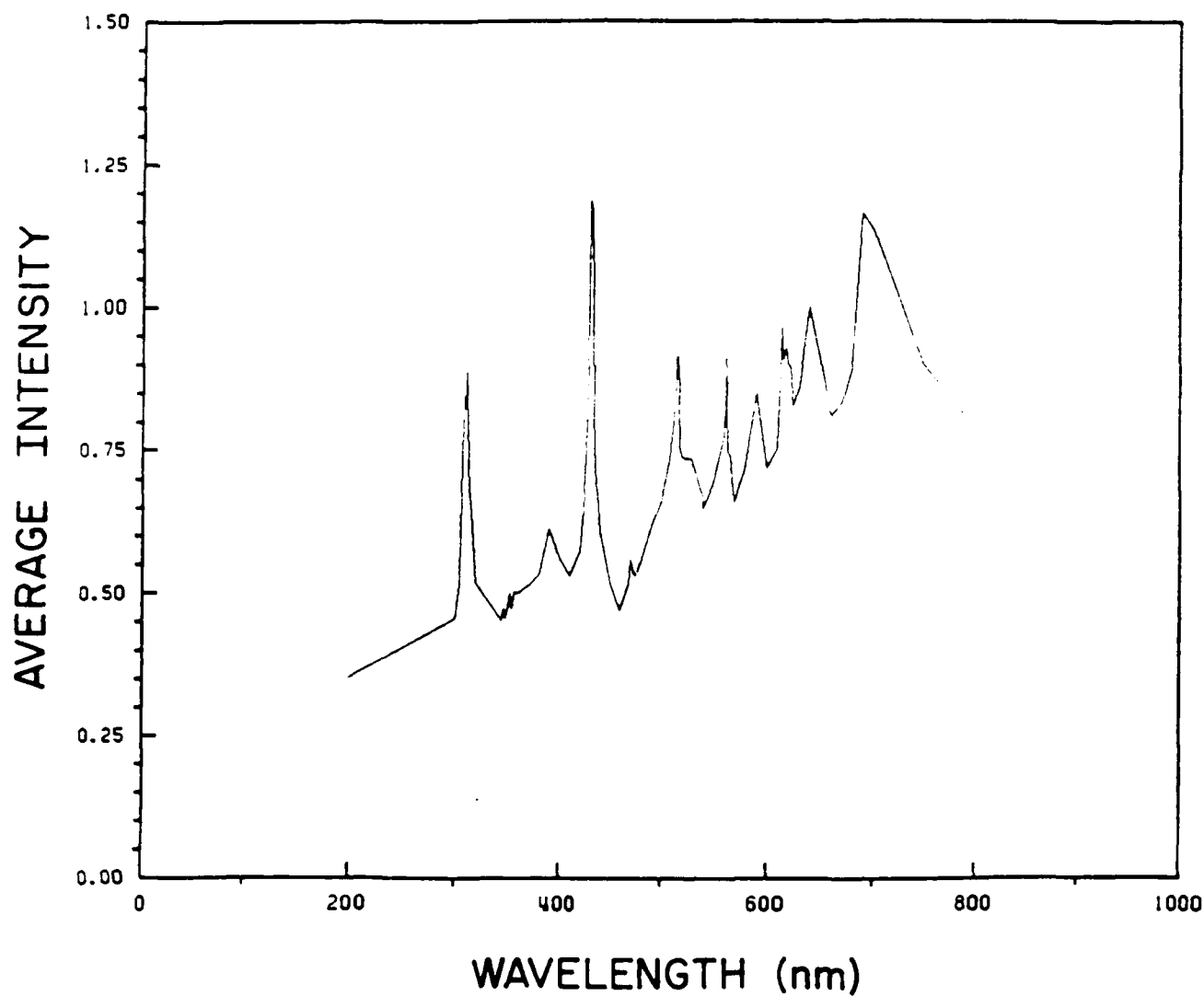


Figure 5. Average signal intensity as a function of wavelength. Several peaks are clearly visible, such as the 310 nm peak due to OH and the 430 nm peak due to CH.

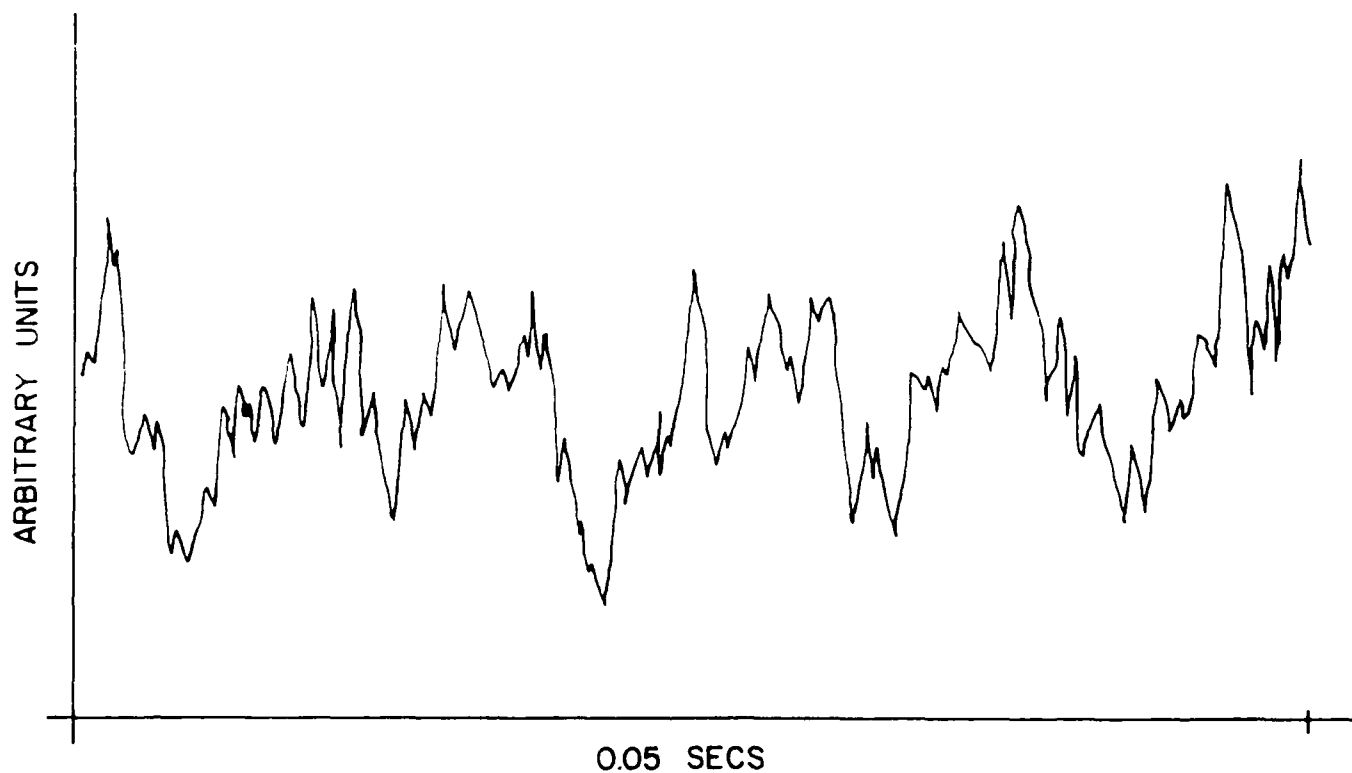


Figure 6. Signal intensity as a function of time. The monochromator is set on the peak at 310 nm, and the graph spans a total time interval of 0.05 seconds.

way to view this information is in the frequency domain. The photomultiplier tube output is processed by a Hewlett-Packard spectrum analyzer, which Fourier transforms the signal into a function of frequency. A typical result ("flicker spectrum") is shown in Figure 7. This spectrum is a potential source of information about the flame and some preliminary surveys have been reported.^{6,7} The bench-top flame monitor built at MSU is equipped to record and analyze this signal, both in the time domain and in the frequency domain.

One limitation of most optical sensors concerns spatial resolution. Although the field of view of a sensor can be limited to a very small angle, the sensor will still detect any light emitted along a line extending from the sensor to the wall. In multiburner boilers, this creates difficulties distinguishing the flame at one burner from the flames at others. To resolve this problem, the MSU flame monitor incorporates a technique known as cross-correlation.^{8,9}

The cross-correlation technique uses two sensors arranged so that their lines of sight intersect at a point (Figure 8). If the flame fluctuations are random and due to turbulence, then the flickering from one part of the flame should be independent of the flickering in another part. Thus, by computing the correlation between the two signals, the flickering originating from the region of intersection can be isolated.

As used in the past, the cross-correlation technique calculated the correlation by averaging in the time domain and obliterated any frequency information in the data. The MSU flame monitor uses a spectrum analyzer to compute a correlation function of frequency.¹⁰

The effectiveness of the cross-correlation technique can best be seen in Figure 9. This figure was produced by vertically translating one channel so the two lines of sight no longer intersect. When this is done, the level of correlation rapidly decreases. Figure 9 demonstrates that the spatial resolution of the system is on the order of one-tenth of an inch.

The experimental flame monitor described above has been built and tested on a bench-top methane-air burner. This system consists of two identical optical systems which use monochromators to select a given wavelength and photomultiplier tubes to convert the light into an electrical signal. A spectrum analyzer Fourier transforms the signals and transmits the results to a COMPAQ microcomputer. The signal can also be read in the time domain by an analog/digital converter connected

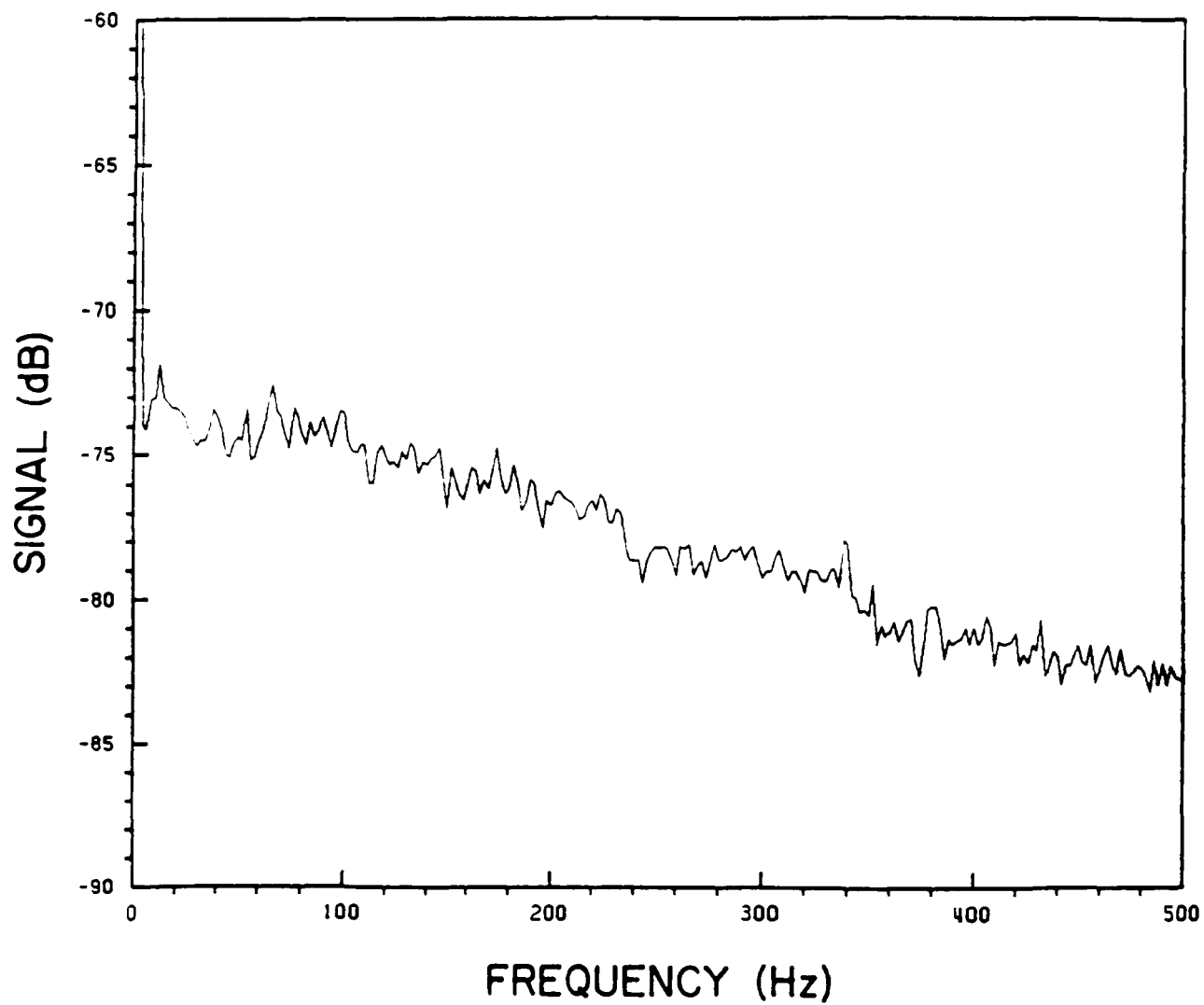


Figure 7. The time-varying signal has been Fourier transformed into the frequency domain.

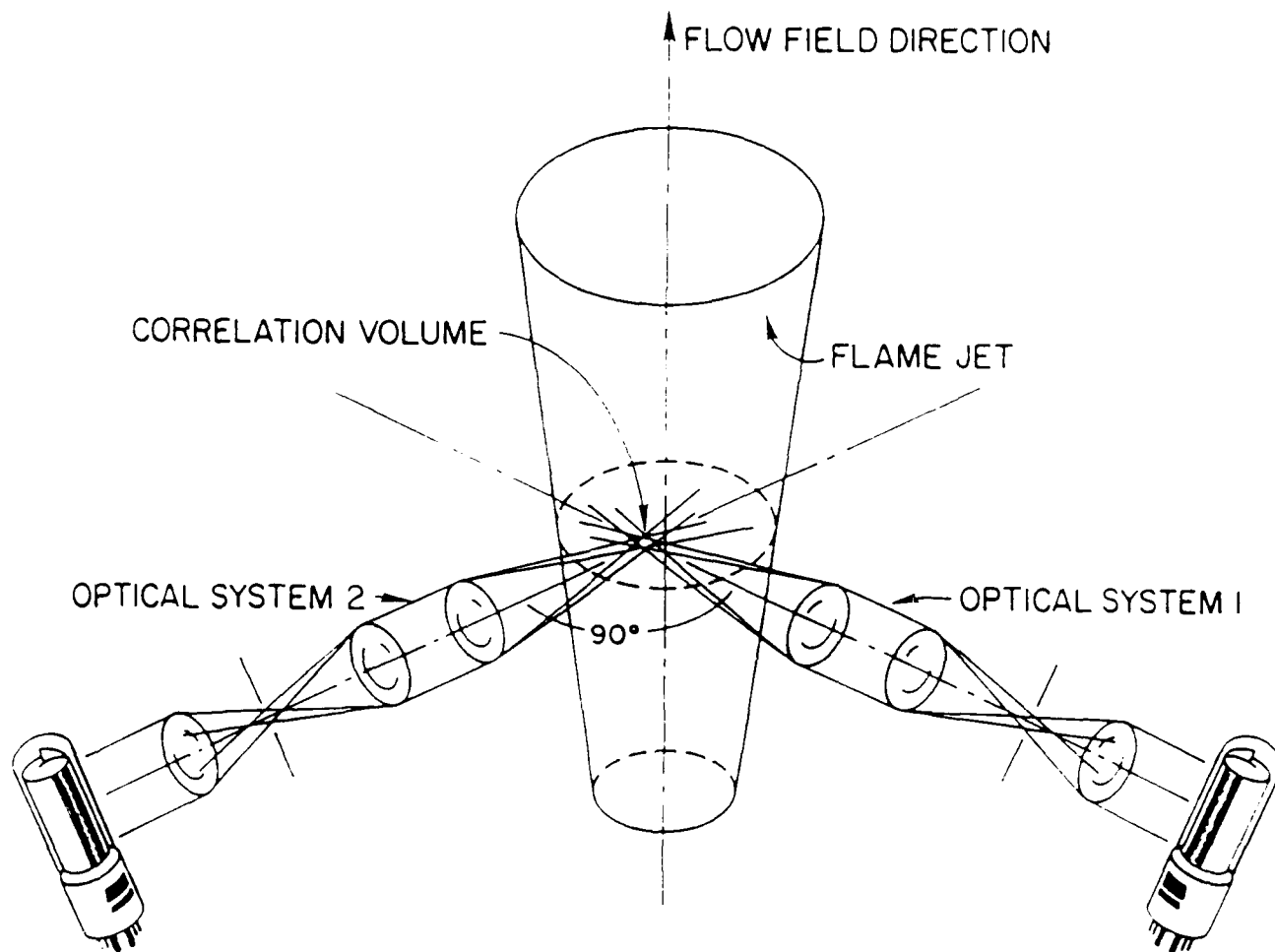


Figure 8. Optical arrangement for the cross-correlation technique.

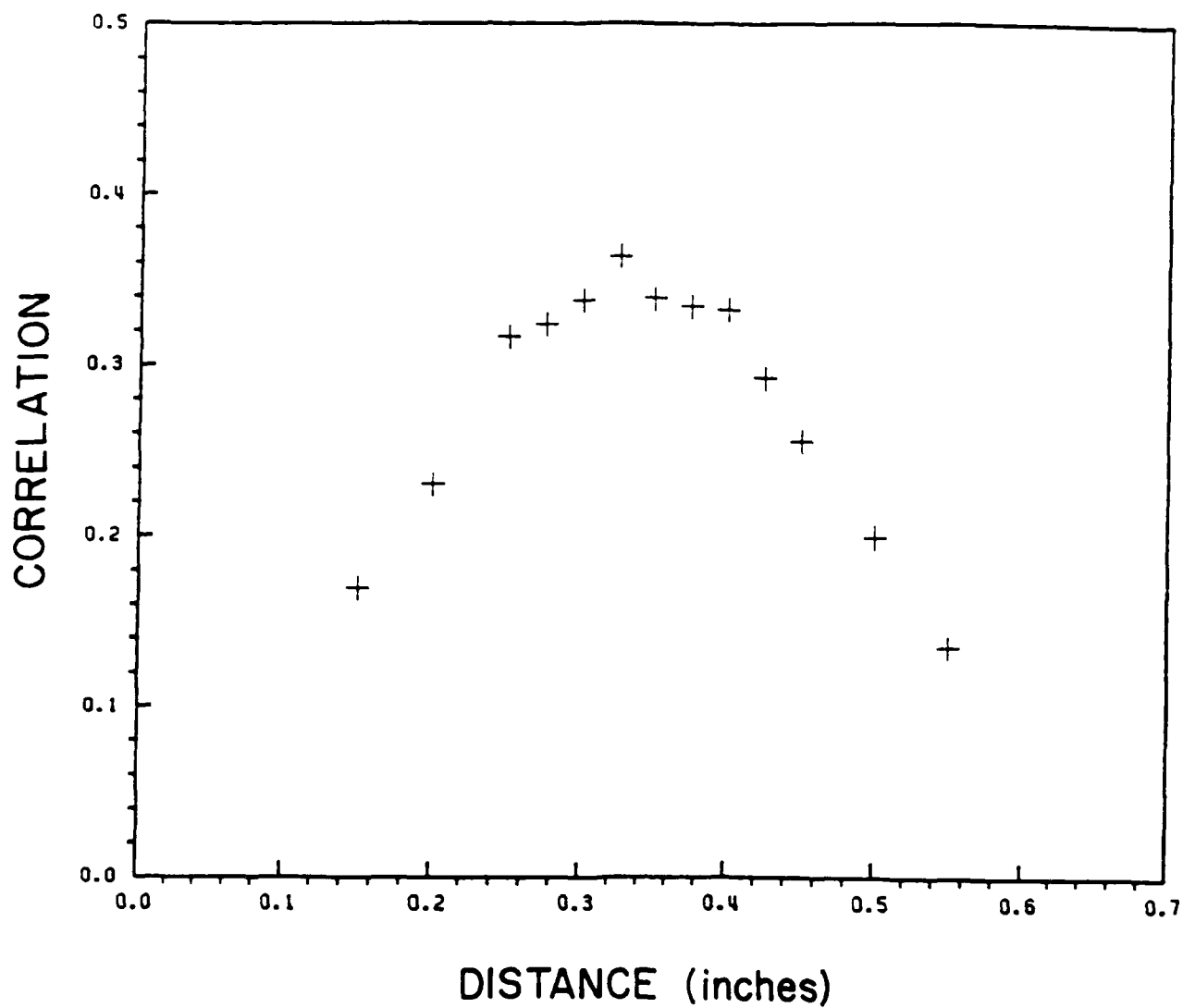


Figure 9. Correlation between the two signals over a frequency range of 400-500 Hz. Misalignment is intentionally produced by translating one channel vertically so the two lines of sight do not intersect. The width of the maximum indicates the spatial resolution of the system.

to the computer which processes and stores the data. Thus, a very powerful and very general flame monitor has been built. With it, every aspect of the light emitted by a flame can be examined with excellent spatial discrimination.

The next step in the investigation is to examine typical fuel oil flames. The MSU/MHD combustion test stand was used for this phase of the project. The test stand is refractory lined, with an internal diameter of eight inches. Fuel oil and air (nominal flow rates 30 and 500 lbm/hr, respectively) are injected at one end.

Soot Temperature Measurements: With a small monochromator in place in the optical arms of the cross correlation experiment, it is also possible to monitor the emission spectrum of the flame over the ultraviolet and visible wavelengths. Since the visible emission of the flame has traditionally been used by experienced human operators to assess flame characteristics, it was considered worthwhile to study the possibility of determining the relationship between the emission spectrum and the air/fuel ratio in a fuel oil flame.⁵ Initial data obtained from the test stand indicated that the emission spectrum of a fuel oil flame is dominated by a continuum rather than discrete emissions from individual combustion products (radicals). The continuum has been attributed to emission by hot soot particles, and the presence of the soot reflects upon the air/fuel ratio. It was hoped at the outset that conditions other than the air/fuel ratio would have a relatively minor influence on the emission.

The monochromator drive (wavelength scan, 300-750 nm) was connected to a computer-controlled stepper motor, and the output of the photomultiplier tube detector was returned to the COMPAQ computer through an analog-to-digital converter (ADC). It was also necessary to signal-average in order to improve the signal-to-noise ratio of the emission spectrum. In order to obtain quantitatively useful intensity information it was necessary to calibrate the monochromator/detector system with sources of known intensities. For the 400-800 nm and 250-600 nm ranges, a 1700 K blackbody source and a quartz tungsten-halogen lamp, respectively, were used. (The uncertainty in the derived temperatures was approximately 50 K.)

Air/fuel ratios ("equivalence ratios"), ϕ , of 0.85, 0.95, 1.05, 1.15, 1.25, and 1.50 were used, and for certain experiments, the gas flowrate in the test stand was also varied. Data were taken through the ports labeled A, B, and C

in Figure 10, and typical emission spectra for two air/fuel ratios are shown in Figure 11. The fuel-rich spectrum indicates a color shift toward the red as compared to the fuel-lean spectrum.

The theory which relates emission, absorption, and scattering of light by the soot particles simplifies for the case where the particle diameter is much smaller than the wavelength, and this condition is met for wavelengths longer than approximately 400 nm in this case. Consequently, a plot of the logarithm of an intensity-wavelength term versus a constant/wavelength gives a straight line with a slope of $-1/T$, as shown in Figure 12.¹¹ The deviation from linearity is observed for wavelengths shorter than 400 nm. (An additional factor in this wavelength region may be the discrete emission of OH at 310 nm.) For a given air flowrate, the temperature of the soot (as determined above) rose as the air/fuel ratio increased. A similar trend was observed at each air flowrate. However, the temperature decreased as the air flowrate increased (for a fixed air/fuel ratio), but this effect was much less pronounced than the effect of varying the air/fuel ratio. The atomization pressure of the fuel was found to have no significant effect as long as there was sufficient air flow to atomize the fuel.

Comparing soot temperatures measured at ports A, B, and C under the same conditions indicated that the temperature of the soot cloud increased in the downstream direction. If the soot temperature increases as the residence time is increased, the variation of soot temperature with flowrate would be explained. These results are consistent with those obtained using a benchtop burner.¹¹

The results of the experiments conducted on the fuel oil-fired test stand indicate that soot particle temperatures are lowest for fuel-rich flames and increase as the air/fuel ratio increases. The temperature is also dependent (to a lesser extent) upon the air flowrate, but with proper calibration and regular monitoring, the soot temperature measurement can be used in a quantitative way to determine air/fuel ratios. In so doing, a single diagnostic system can be used to monitor multiple characteristics of a boiler flame.

Infrared Spectroscopy

HeNe Differential Infrared Hydrocarbon Monitor: A differential infrared absorption method is being developed primarily to monitor unburned hydrocarbon vapors in a Navy boiler. The technique uses two helium-neon (HeNe) lasers operating at different infrared wavelengths and compares the absorption of

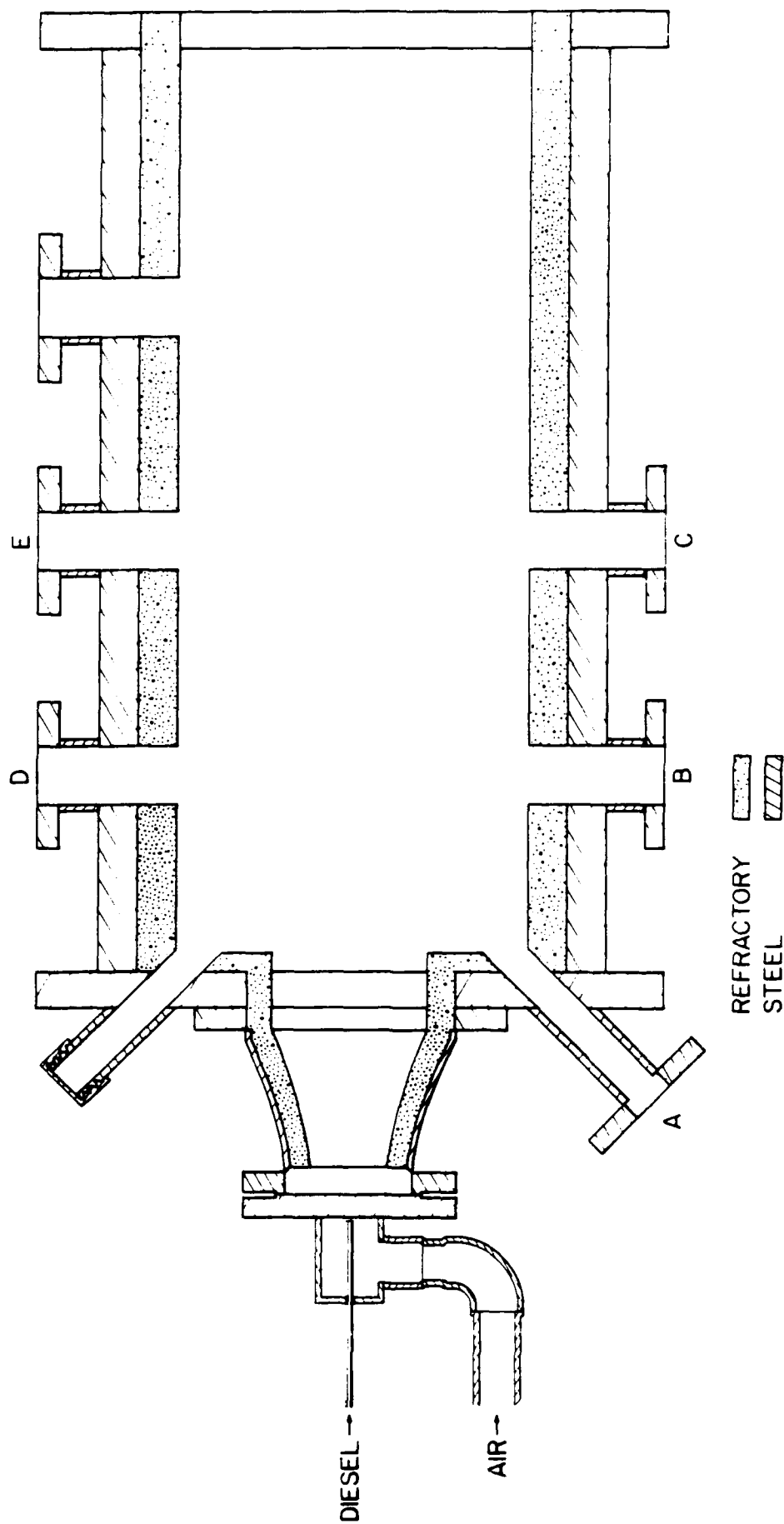


Figure 10. A longitudinal cross section of the combustor and the boiler simulator section. Optical ports labeled A, B, and C were used.

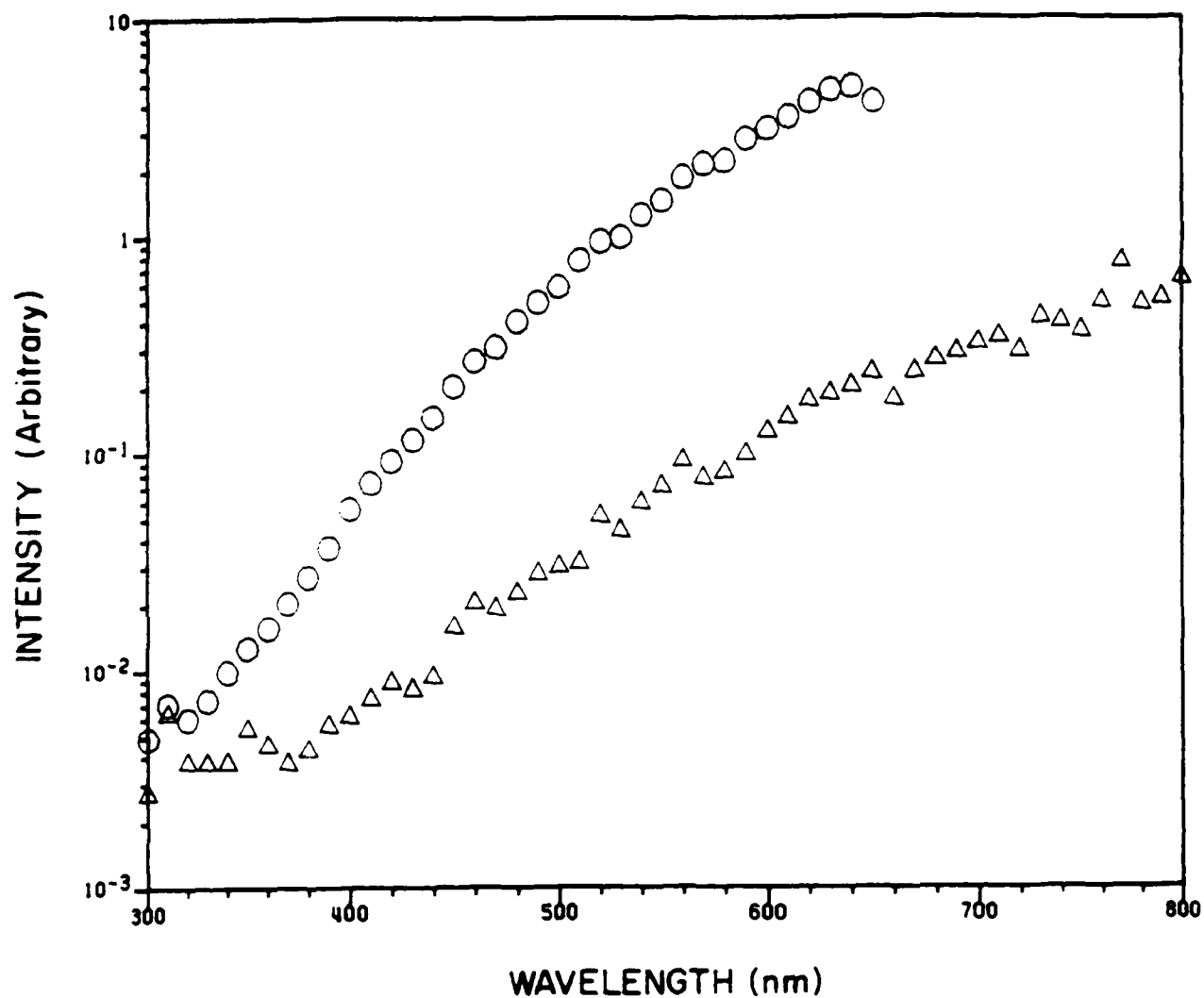


Figure 11. Relative radiation intensity as a function of wavelength for two different equivalence ratios. The circles are $\phi = 0.85$ (fuel-rich), and the triangles are $\phi = 1.25$ (lean).

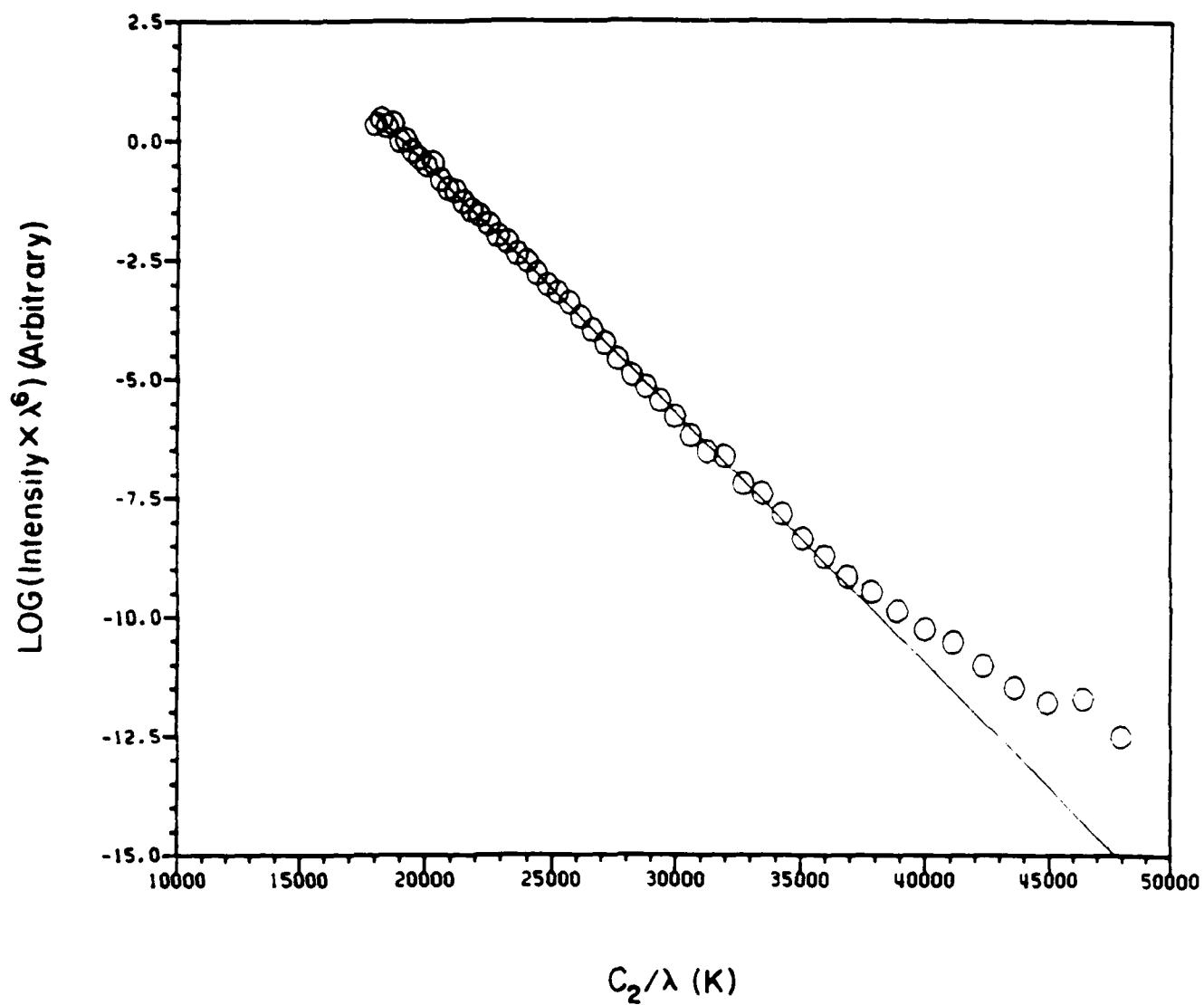


Figure 12. Experimental spectrum transformed into $\log(I/\lambda^6)$ versus C_2/λ coordinates. The slope of the line yields a soot temperature of 1910 K for $\phi = 1.05$ and an air flow rate of 450 lb/hr.

hydrocarbons at these two wavelengths. In a HeNe laser, the most efficient of the neon emissions in the 3.39 μm wavelength range is the $3s_2-3p_4$ transition at 3.3922 μm (2947.9 cm^{-1}). The inclusion of a sample of methane within the optical resonator (intracavity) of a HeNe laser alters the output to that of the $3s_2-3p_2$ transition at 3.3911 μm (2948.9 cm^{-1}).¹² The difference in the absorption at these two wavelengths can be related to the concentration of hydrocarbons in the optical path.¹³

In the experimental layout shown in Figure 13, the two laser beams pass through a chopper which typically operates at 2 kHz. Laser 2 operates at 3.3911 μm (shifted), while laser 1 operates at 3.3922 μm (unshifted). In each beam a quartz plate sends approximately 10% of the beam to a detector which is used to monitor laser stability. The remainder of each beam travels on, and the two beams are rendered collinear at a ZnSe beamsplitter. The refractive index of ZnSe is sufficiently high that an ordinary window can be used for this purpose. At this point the beams can be directed to a sample cell or a combustion chamber then onto a liquid-nitrogen-cooled indium-antimonide (InSb) detector. The detector signal is amplified and sent to a lock-in amplifier (tuned to the chopper frequency) where phase sensitive signal processing occurs. Typically, the two lasers have a phase mismatch of 90°. The lock-in amplifier has RS-232 and IEEE data buses which facilitate connecting the COMPAQ microcomputer to the system.

For the 26 cm intracavity cell in use at the present time, methane pressure between 120 and 140 torr offers optimal conditions. If the methane pressure is less than 120 torr, the wavelength shift is not sufficient, but if the pressure is greater than 140 torr, the absorption is so strong that the laser gain is low and the noise of the laser is unacceptably high. An additional factor to consider is the wavelength stability of the laser. When the sample cell contained low total pressures of gases such that the pressure broadening was minimal, an oscillating signal was obtained presumably because of slight wavelength variations which brought the laser into and out of resonance with the methane sample gas. With total pressures (methane plus nitrogen or air) near atmospheric, the oscillations were not observed.

The sensitivity of the system is indicated in Figure 14, which illustrates the deflection caused by 0.2 torr of methane in a 10 cm sample cell. At the

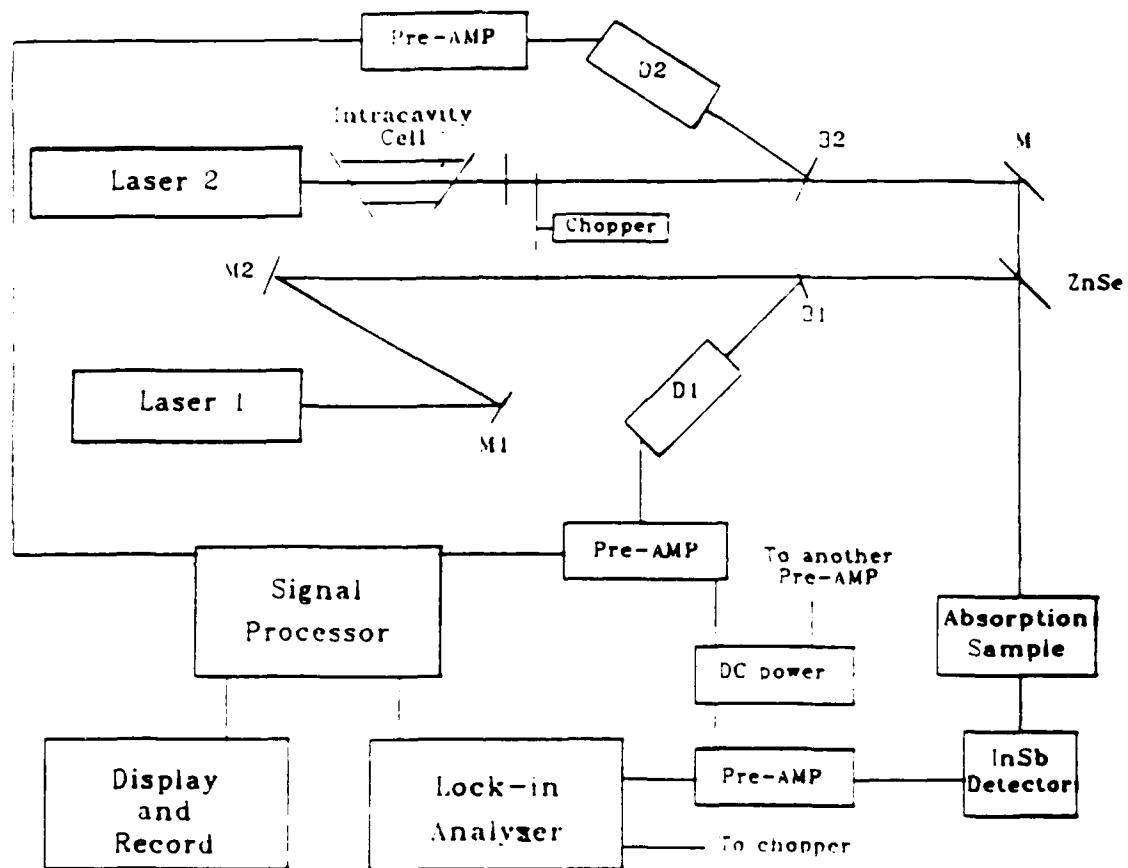


Figure 13. Schematic diagram of the HeNe differential infrared (hydrocarbon) monitor.

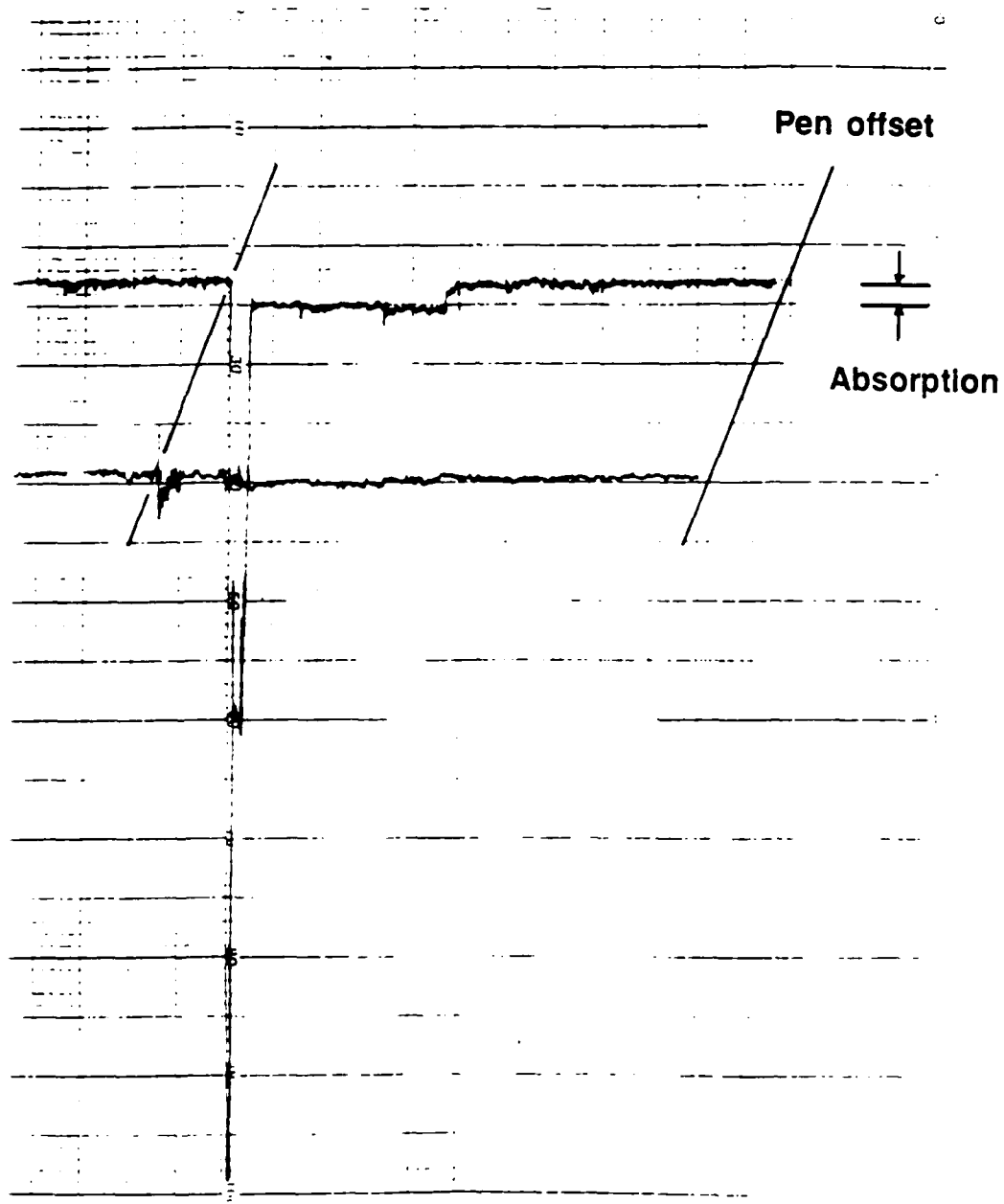


Figure 14. Experimental data record showing the absorption by 0.2 torr methane in a 10-cm cell. (Upper curve is for laser 1; lower curve is for laser 2.)

other extreme, 10 torr of methane completely absorbed the laser output. With the sensitivity and stability of the system adequately determined in a laboratory setting, various practical tests were devised.

For example, in a conventional laboratory burner, the system was used to monitor the lateral distribution of methane in a fuel-rich flame. Using ambient air as the oxidizer, a distribution such as that shown in Figure 15a was observed. When air was also brought through a tube in the center of the burner, a somewhat different distribution was observed (Figure 15b). Understandably, the concentration of methane was slightly lower immediately above the air inlet. In each case, the total displacement over which methane was detected was approximately 4 cm.

The system was also transported to the combustion test facility at DIAL. The laser beams were directed across an 8-inch section of the test stand through an optical port to the InSb detector on the other side. Nitrogen gas was used to purge the windows. Figure 16 shows the results of measurements made for a variety of methane percentages with two different air flowrates. Each data set is a straight line as expected, and the detection scales quantitatively for the two air flowrates. Similar curves were obtained for a fixed flowrate with variable gas temperatures. These data show differences which are consistent with the temperature dependence of the rotational transition of methane being detected.

The techniques described above may also be applied to the detection of higher hydrocarbons. Because methane is a gas with well-characterized properties, it has been useful for evaluating the system. In order to achieve similar sensitivity for higher hydrocarbons, it will be necessary to use the intracavity cell to shift the output of laser 2 farther away from that of laser 1. Other gases have been used, but it is most likely that a mixture of gases will be required for that purpose. An alternative approach is to use the HeNe transitions near $1.15\text{ }\mu\text{m}$ to probe the overtones of the hydrocarbon vibrations. Similarly, it may be useful to investigate the possibility of using diode laser sources in this near infrared region where readily available optical fibers have their maximum throughput.

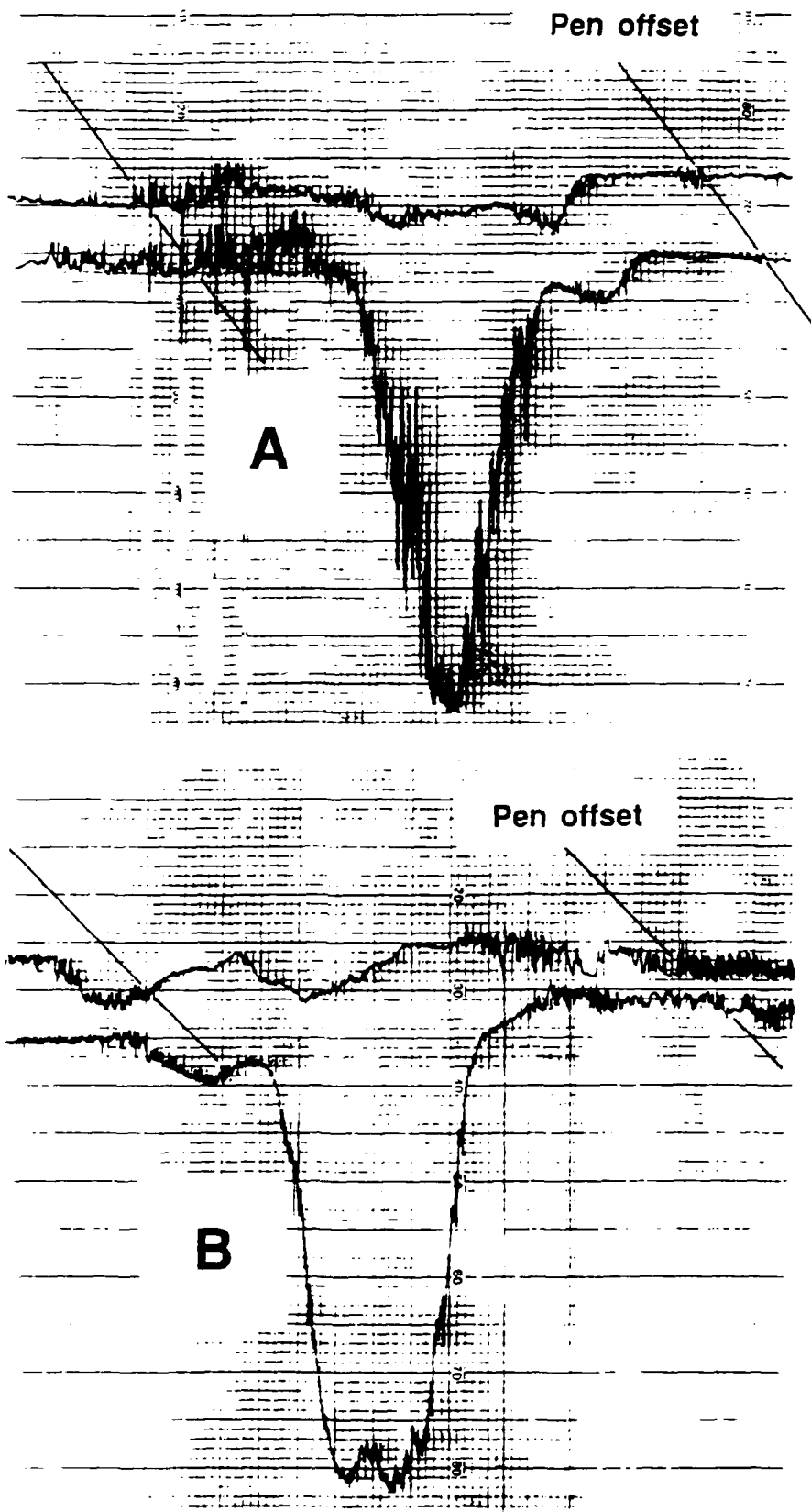


Figure 15. Methane concentration distribution in a bench-top methane flame: (A) combustion using ambient air, and (B) combustion using the air inlet of the burner. (Upper curve in each section is for laser 2; lower curve is for laser 1.)

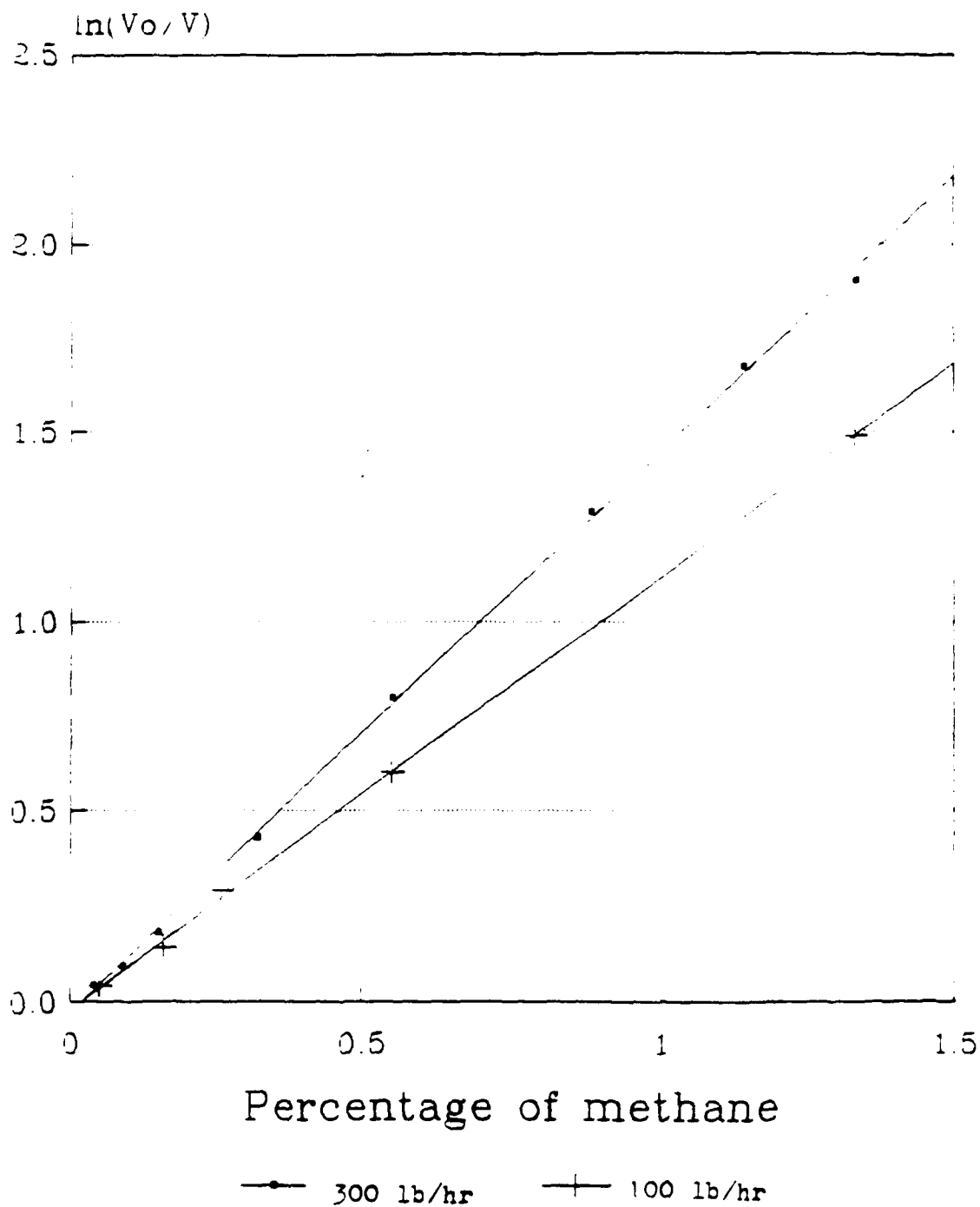


Figure 16. Absorption of methane in the test stand at different air flow rates (300 lb/hr and 100 lb/hr).

Diode Laser CO/CO₂ Monitor: The CO/CO₂ ratio in the combustion gases of a Navy boiler is intimately related to the safe and efficient operation of the boiler. Present systems, using gas sampling or nondispersive infrared techniques, are slow and stack-based. Infrared laser-based methods are being developed to provide rapid, burner-specific measurements of this important ratio. Initially, semiconductor diode lasers operating near 4.7 μm (2100 cm^{-1}) and 4.3 μm (2300 cm^{-1}), specifically coincident with CO and CO₂, respectively, were envisioned for this project.¹⁴ However, current activity in our laboratory is concentrated on a 4.5 μm diode laser which should be absorbed by both CO and CO₂.

Diode lasers emit two or more closely-spaced lines (10^{-4} cm^{-1} linewidths) which are tunable over their intrinsic bandwidths of 15 - 100 cm^{-1} . Unfortunately, the tuning, which is controlled by temperature in the range of 15 - 45 K and current between 0.2 and 0.9 μamps , is both nonlinear and noncontinuous. After taking many survey scans of CO and CO₂ absorption spectra, it was found that it was necessary to scan very slowly (0.2 $\text{cm}^{-1}/\text{min}$) over narrow ranges (approximately 2 cm^{-1}). The use of a marker etalon, with a free spectral range of 0.049 cm^{-1} , is also required to provide a continuous wavelength calibration and to indicate when discontinuities, or "mode hops", occur in the spectra. After much experimentation, many of the CO₂ lines but none of the CO absorption features which are in the range of this 4.5 μm diode have been identified.

The current emphasis is to empirically find the best operating conditions and spectral ranges of this laser for CO/CO₂ measurements. For any wavelength desired, there are many combinations of temperature and current possible, and all of these must be examined to determine the optimum operating parameters. There are also several wavelengths which can be used for CO/CO₂ monitoring, and these will also have to be carefully studied to find the best overlap of good laser operating characteristics and the spectral and concentration properties of the CO and CO₂ absorptions. The above infrared diode laser instrument is bulky, so the bench-top fuel oil burner will be necessary for testing.

Contributing to the bulkiness (and cost) are the closed-cycle helium refrigerators (cryostats) required for cooling the lasers and detector. Progress is being made in the design of smaller and more efficient laser sources in this area, but it may be some time before they become practical. One alternative is to use existing room-temperature semiconductor lasers operating in the 1.5 μm region, which overlaps with stretching overtones. These lasers do not require

low temperature cooling devices and also have relatively good output powers (as much as 1 Watt CW). The only drawback to this possibility is that the absorption coefficients for CO and CO₂ overtones in this region are greatly reduced relative to their fundamentals.

Additional work would be needed to parameterize the operation of all the existing diodes and determine the best approach for proceeding with the development of the CO/CO₂ monitor.

Auxiliary Instrumentation

Bench-Top Fuel Oil Burner: At present two types of combustion devices are used in the development of combustion diagnostic instruments. The availability of a bench-top fuel oil burner would help fill the gap between the Bunsen burner and the oil-fired test stand. This type of burner would speed up the development process for instrumentation and save part of the time and money required to operate the test stand. Many tests could be done on the bench-top that would otherwise have to be done on the test stand.

The basis for this burner is an ultrasonic atomizing nozzle that was bought from the Sonotek Corporation. The advantage of an ultrasonic atomizer in this application is that no high air or fuel pressure is needed. This nozzle works well in its specified operating range of up to approximately 0.25 gpm. Fuel oil passes through the nozzle and exits from its tip in a cloud of droplets of about 30 micron diameter. Ideally these droplets will be entrained in the air flow in the burner throat for a time sufficient for good mixing before exiting to the mouth of the burner.

Several problems were encountered during initial attempts to develop a burner. One of the main problems was the cost of the atomizer and its temperature limitations. The atomizing nozzle was always kept at a safe distance from the flame region of the burner. This resulted in good fuel/air mixing but created a problem with fuel droplets adhering to the burner walls. This resulted in the eventual collection of fuel in the air supply line.

A related problem occurred when a screen was placed across the burner mouth. Fuel droplets stuck to the screen and collected in larger drops in some portions of the screen. The flame would not attach to the screen and was not very stable. Burning was confined to a very narrow range of fuel flows.

Proceeding on the assumption that additional energy had to be added to the flame, the burner shown in Figure 17 was constructed. A helical nichrome spring covers the mouth and acts as an attachment point for the flame. About 20 volts is applied to the nichrome wire to start the burner. After the flame starts the voltage is removed, the nichrome remains red hot, and the flame is stabilized. All fuel reaching the burner mouth is atomized on the hot surface of the nichrome. The range of useful air/fuel flows is extended to the limit of the atomizing nozzle.

A peristaltic pump with a 12-roller head to minimize flow pulsation was added to the burner. It replaced the simple gravity-feed system which was initially used to deliver fuel to the burner, and it has noticeably improved the operation of the burner. The burner was packaged with the pump to make it convenient for use in the laboratory. As feedback from these tests is received, modifications to the burner will be made. For example, air and fuel flow metering are being added. The current version, however, has the problem of fuel sticking to the walls, and it remains to be seen how this will affect diagnostic testing.

Explosion Test Cell: The Explosion Test Cell (ETC) shown in Figure 18 is a cylindrical pressure vessel which was designed to accomplish two primary objectives--to contain an air/fuel mixture at elevated temperatures and to allow the determination of flammability limits of hydrocarbon fuels, Diesel Fuel Marine in particular. The ETC has been described in detail elsewhere² and will not be described here except to say that it is instrumented with thermocouples and a pressure transducer.

Work on the determination of flammability limits for Diesel Fuel Marine (DFM) continued but difficulties still exist. The procedure by which flammability limits are to be determined consists of heating the ETC to a predetermined temperature, injecting the liquid fuel, agitating the fuel/air mixture, and extracting a sample for analysis by an HP 5830A Gas Chromatograph (GC). Following the GC analysis, more fuel or air should be added to the ETC to attain a desired air/fuel ratio. After the desired air/fuel ratio has been attained a spark is generated inside the ETC to ignite the air/fuel mixture. This process is repeated until an air/fuel ratio is found which is flammable but for which an air/fuel ratio that is slightly leaner is not flammable. This ratio is the lower flammability limit at the stated temperature for the fuel.

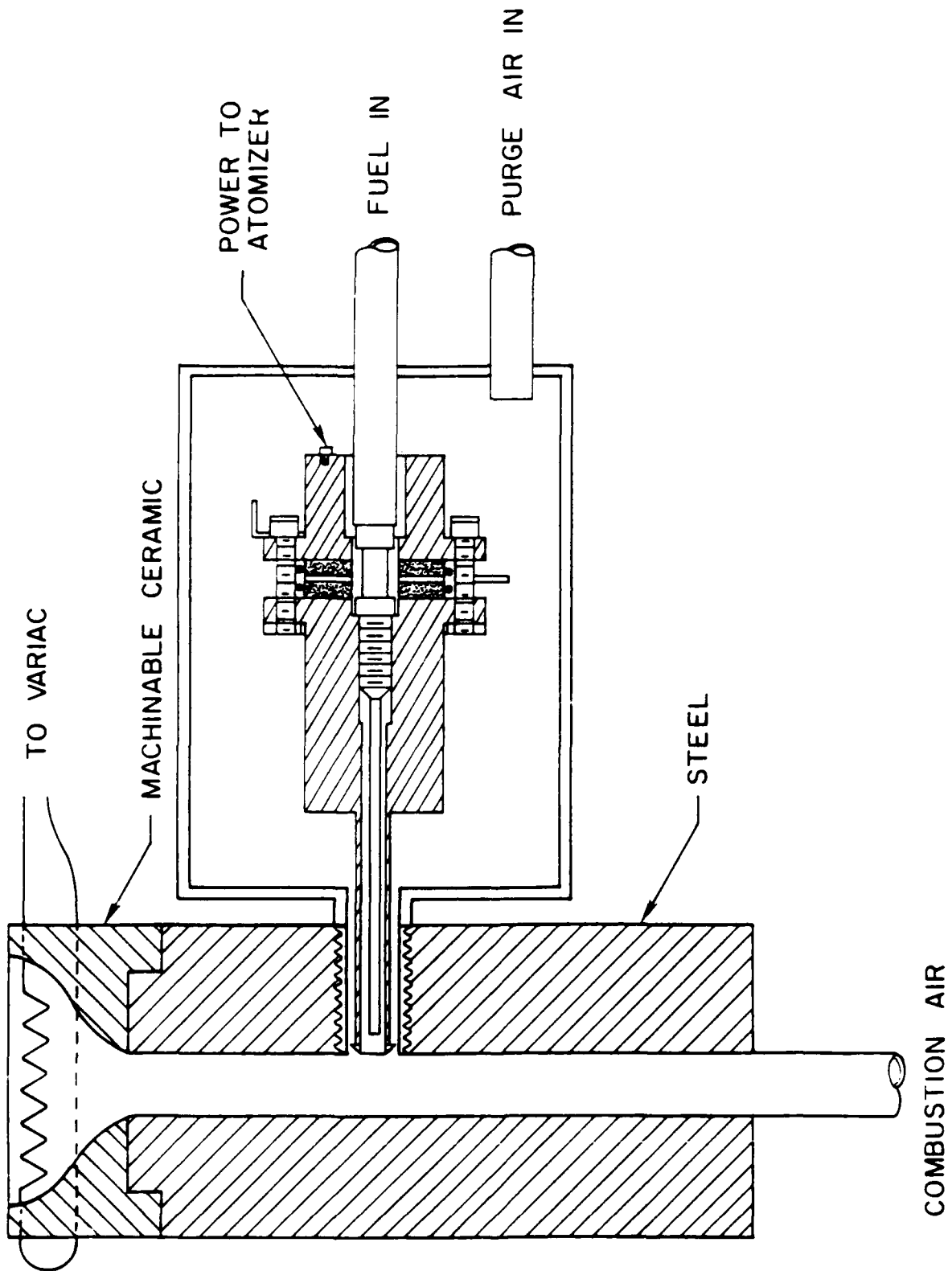


Figure 17. Bench-top fuel oil burner.

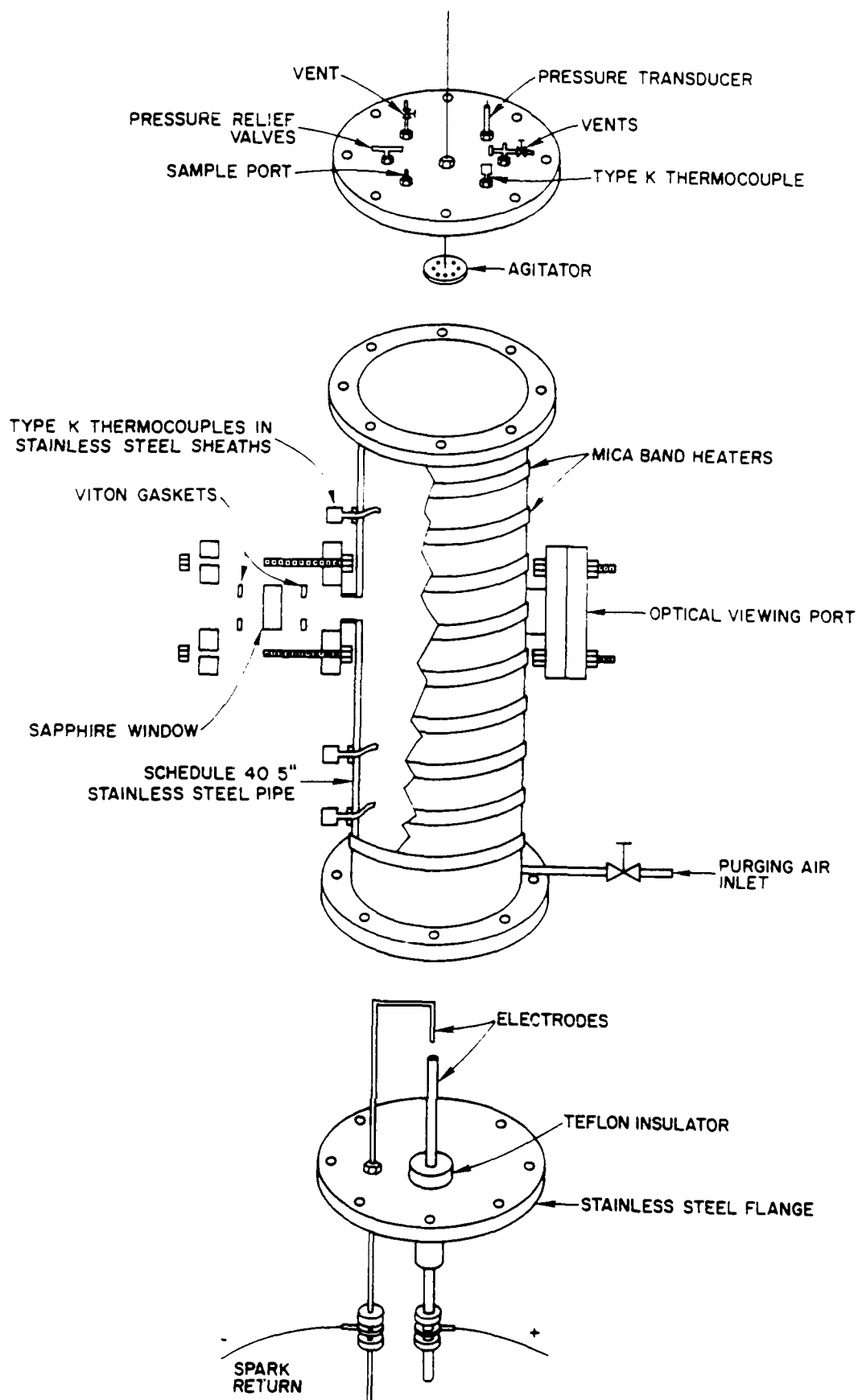


Figure 18. Detailed diagram of the explosion test cell.

The main problem with this process is that during GC analysis some of the fuel vapor is slowly oxidizing in the ETC so that by the time the GC analysis is done the reported concentration is no longer valid making an adjustment to the concentration impossible. An additional effect of this slow oxidation is that there is no longer a mixture of fuel and air but of fuel, oxidized fuel components, and air. This means any flammability limit determinations will not truly reflect an air/fuel ratio.

An alternative method of analyzing post combustion gases was found but does not appear to have an advantage over the old way. As reported in the 1986 report analysis of O₂, N₂, CO, and CO₂ was done on two parallel columns of Chromosorb 102 and Molecular Sieve 5A.² The new method consists of using two independent columns of Molecular Sieve (MS) 5A and Porapak Q with each column requiring a separate injection and detector port. This precludes the possibility of doing fuel/air and post-combustion gases separation within a close time frame of each other since the GC only has two injection and detector ports. Operation of the Molecular Sieve 5A and Porapak Q columns in parallel proved unsatisfactory. Splitting of the flow between the columns was unsatisfactory and produced inconsistent results. The use of the MS 5A and Porapak Q columns in parallel has advantages since they can separate the O₂, N₂, CO, and CO₂ in about nine minutes, a marked improvement over the 14 minutes required for the MS 5A/Chromosorb 102 combination.

Preliminary work on the derivation of a relationship between rate or pressure rise and flame speed in the ETC was begun and it appears the derivation will not be as simple as initially thought. Work will continue on this derivation.

Gas and Liquid Chromatography: Fuel analysis is performed by using chromatographic methods. Because of the intrusive nature of these experiments, they are not used as on-line monitors; instead, they are useful for calibrating the nonintrusive techniques being developed.

A Hewlett-Packard 5830A gas chromatograph (GC) fitted with thermal conductivity detectors is used for analyzing hydrocarbons in fuels and for analyzing the extent of deflagration in the explosion test cell. To separate and monitor H₂, O₂, N₂, CO, CO₂, and very light hydrocarbons (C₁ - C₄), two columns packed with Chromosorb 102 and Molecular Sieve 5A have been operated in parallel. Recently, a commercially available column simplified the procedure of operating these two columns in parallel by combining the two in a concentric fashion. One

material is packed in a 1/8-inch column which is placed inside a 1/4-inch column packed with the other material. By combining the Chromosorb and Molecular Sieve columns, the other injection port and detector are free for another column whose choice would depend upon the specific problem. For example, an OV-17/QF-1 column is used to separate higher hydrocarbons (C₆ - C₂₂), whereas Porapak columns might be used for separating specific gases more efficiently. In the event that higher sensitivity or chromatographic resolution were required, flame-ionization detectors and 0.25-mm fused-silica capillary columns are available in adjacent laboratories.

The Waters high performance liquid chromatography (HPLC) system with refractive index (RI) and ultraviolet (UV) absorption detection is available for separating liquid fuel oil into its components or determining aromatic/aliphatic ratios. Typically, hexane is used as the solvent for such an analysis in a 5 μ m silica column.

CONCLUSIONS

The completed work which is summarized herein and the work which is anticipated for the future constitute a comprehensive program to develop monitoring devices which can eventually be incorporated into the control system of a naval boiler. Each of the individual projects has passed the prototype stage, and with the completion of the bench-top fuel oil burner, many tests which would otherwise have required considerable time and expense in operating the combustion test facility (CTF) may be accomplished in a laboratory setting. Moreover, these tests can help optimize instrument conditions for field tests at the DIAL test stand or at a boiler simulator off-campus. Most of the instruments are portable, even though they are not yet as compact as they might become.

The variety of sensors under development address the problems of safety, but, at the same time, it is probable that the efficiency of Navy boilers can be monitored with these instruments. And while each sensor is being developed for a particular task, the interrelationships of the problems dictate that the signal from one sensor will be important for understanding the signal from another. For example, a fuel-rich flame will alter both the frequency spectrum of the cross-correlation experiment and the absorption spectra of the differential infrared (hydrocarbon) monitor and the infrared diode laser (CO/CO₂) system. This complementary nature of the data will allow problems to be solved more efficiently. Additionally, the process of developing these instruments and the recent advances in technology have indicated alternative approaches to the problems at hand. Possibilities which exist today even suggest modifications to existing equipment which would simplify the sensors and make them more acceptable for applications on a Navy boiler.

Design criteria for each sensor include the requirement that all the sensors be interfaced to a single control unit, and the COMPAQ microcomputer was chosen for the task. A wide variety of software and hardware is available for the COMPAQ, but in a shipboard application, it would very likely be replaced by a newer, faster IBM-PC compatible system. For the present time it is sufficient for developmental purposes, and it can function as a smart terminal for the DIAL VAX 11-780 computer if additional data handling capability is needed.

REFERENCES

1. Yang, L. C. July 1984. Surface-moisture monitoring techniques. *JPL Invention Report* NPO-15494/4971, Jet Propulsion Laboratory, California Institute of Technology, Pasadena, CA.
2. October 1986. Application of remote sensing optical instrumentation for diagnostics and safety of naval steam boilers. Navy Contract #N00014-84-K-0301, Final Report, MHD Energy Center, Mississippi State University, Mississippi State, MS.
3. Wilson, E. S.; John, R. R.; and Summerfield, M. 1957. *Jet Propulsion* 27:892-894.
4. Fuhs, A. E. 1960. *ARS Journal* 30:238-243.
5. McArthur, L.; Lord, H. C.; and Gilbert, L. F. 1977. *ISA Trans.* 16:3:49-54.
6. Brown, R. H., and Glassby, B. 1982. An investigation of the power density spectrum of radiation flickers from oil and coal flames. Central Electricity Generating Board NER/SSD/N335.
7. Harvey, S. M. 1979. Current status of boiler flame scanner research. Ontario Hydro Research Division Report 79-268-K.
8. Kuhnert, D., and Gunther, R. 1975. *J. Inst. Fuel.* pp. 98-103.
9. Noltingk, B. E.; Robinson, N. E.; and Gaydon, B. G. 1975. *J. Inst. Fuel.* pp. 127-131.
10. Carlton, D. C. 1984. The investigation of ultraviolet radiation fluctuations in a turbulent diffusion flame. M. S. Thesis, Mississippi State University.
11. Feugier, A. 1973. In *Heat Transfer in Flames*. Afgan, N. and Beer, J. M., eds. Washington, DC: Scripta.
12. Moore, C. B. 1965. *Appl. Optics.* 4(2):252-253.
13. Grant, W. B. 1986. *Appl. Optics.* 25(5):709-718.
14. Eng, R. S., and Ku, R. T. 1982. *Spectrosc. Lett.* 15:803-805.

•
•
•

APPENDIX

PUBLICATIONS AND PRESENTATIONS

1. Kalasinsky, V. F.; Beiting, E. J.; Shepard, W. S.; and Cook, R. L. 1989. Applications of Coherent Anti-Stokes Raman Spectroscopy and Other Laser-Based Techniques to Combustion Analysis. *Vib. Spec. and Struct.* 17B:173-185. Amsterdam: Elsevier Science Publishers.
2. Norton, O. P. 1989. Soot Temperature Measurements in Fuel Oil Flames. *Proceedings of the ASME Fossil Fuels Combustion Symposium*. Houston, Texas, January 22-25.
3. Zhang, Hansheng. August, 1989. The Detection of Methane with Laser Differential Absorption. M.S. Thesis. Department of Physics, Mississippi State University.
4. Kumar, R. A.; Etheridge, J.; Cook, R. L.; and Shepard, W. S. Performance of a Capacitance-Based Liquid Fuel Oil Sensor. In preparation.
5. Etheridge, J., and Shepard, W. S. Design and Operation of a Bench-Top Fuel-Oil Burner. In preparation.
6. Kalasinsky, V. F.; Zhang, H.-S.; and Cook, R. L. Determination of Infrared Laser Output Frequencies Using Fourier Transform Spectroscopy. In preparation.
7. Zhang, H.-S.; Kalasinsky, V. F.; and Cook, R. L. Detection of Methane in Combustion Gases using Laser Differential Absorption. In preparation.